PHYSICAL REVIEW B **79**, 081101(R) (2009)

High-pressure ^{51}V NMR study of the magnetic phase diagram and metal-insulator transition in quasi-one-dimensional β-$Na_{0.33}V_2O_5$

Taisuke Suzuki,[1] Ichihiro Yamauchi,[1] Yasuhiro Shimizu,[1,2] Masayuki Itoh,[1]
Nao Takeshita,[3] Chieko Terakura,[3] Hidenori Takagi,[4] Yoshinori Tokura,[5]
Touru Yamauchi,[6] and Yutaka Ueda[6]

[1]*Department of Physics, Graduate School of Science, Nagoya University, Furo-cho, Chikusa-ku, Nagoya 464-8602, Japan*
[2]*Institute for Advanced Research, Nagoya University, Furo-cho, Chikusa-ku, Nagoya 464-8601, Japan*
[3]*National Institute of Advanced Industrial Science and Technology, Tsukuba, Ibaraki 305-8562, Japan*
[4]*Department of Advanced Materials Science, University of Tokyo, Kashiwa, Chiba 277-8561, Japan*
[5]*Department of Applied Physics, University of Tokyo, Hongo, Bunkyoku, Tokyo 113-8656, Japan*
[6]*Institute for Solid State Physics, University of Tokyo, Kashiwa, Chiba 277-8581, Japan*

(Received 31 October 2008; revised manuscript received 15 January 2009; published 9 February 2009)

High-pressure ^{51}V NMR measurements are conducted up to 9 GPa using a modified Bridgman anvil cell in a quasi-one-dimensional conductor β-$Na_{0.33}V_2O_5$ which shows pressure-induced superconductivity from a charge order state. We determine the magnetic and Na order transition temperatures and construct the phase diagram of the metal-insulator transition in β-$Na_{0.33}V_2O_5$. We demonstrate that the antiferromagnetic long-range order phase persists up to a critical pressure $P_c \sim 8$ GPa where the charge order completely melts. The local spin susceptibility shows distinct site dependence and a crossover from a Curie-Weiss one-dimensional liquid to a Fermi-liquid metal with enhanced density of states above P_c.

DOI: 10.1103/PhysRevB.79.081101 PACS number(s): 71.30.+h, 76.60.−k, 75.50.−y, 75.40.Gb

Mapping electronic states in a thermodynamic phase diagram offers a starting point to understand metal-insulator transitions (MITs) occurring on strongly correlated electrons. In many transition-metal oxides and organic conductors, superconducting states emerge on the verge of MIT from Mott insulators with antiferromagnetic (AF) long-range order as a function of band filling or width.[1] Metals on the verge of MIT have anomalous features such as the effective-mass enhancement and pseudogap behavior. It has been a long-standing issue whether the interplay between spin and charge is essential for the emergence of unconventional metals and superconductivity. Thus it is important to investigate MIT phase diagrams with various ordered phases and without any orders. In this context, superconductivity appearing from the charge order phase has attracted much attention in β-$A_{0.33}V_2O_5$ (A=Na^+, Li^+, and Ag^+) where charge fluctuations might be relevant to low-energy properties.[2,3]

β-$Na_{0.33}V_2O_5$ is a quasi-one-dimensional (1D) conductor, as evidenced from the dc and optical conductivities.[4–7] In spite of the complex crystal structure consisting of three crystallographically independent V sites, the unit of the electronic structure can be effectively regarded as three sets of two-leg ladders,[8–10]—two V1-V3 ladders and one V2-V2 ladder as illustrated in Fig. 1(a). In a limit of the strong rung coupling, the electronic structure is further simplified into weakly coupled three chains.[11] The nominal V valence ratio is V^{4+}:V^{5+}=1:5, i.e., only 1/6 average electron in a nondegenerated t_{2g} orbital.[8] A first-order MIT occurs at T_{MI} =135 K accompanied by charge ordering as evidenced by NMR,[12,9,10] neutron,[13] and x-ray diffraction measurements.[14] However, the charge order pattern proposed experimentally is not a simple Wigner crystal. The spin sector remains paramagnetic even below T_{MI} and finally exhibits the Néel order at T_N=24 K.[4,9,15,16] Despite metallic conduction along the ladder direction above T_{MI}, the magnetic susceptibility follows the Curie-Weiss law with an antiferromagnetic Weiss temperature, −163 K. Site dependence of the Curie constant suggests that the charge density is not uniform even in the metallic state.[10] In addition, the nuclear spin-lattice relaxation rates depend on the three V sites and exhibit spin-diffusion behavior.[17,18]

The resistivity measurement under pressure has revealed the overall pressure-temperature (P-T) phase diagram up to 10 GPa.[2,3] The superconducting phase appears abutting on the charge order insulating phase above 7 GPa. However, the nature of the insulating and metallic phases, possibly relevant to superconductivity, is poorly understood due to the lack of magnetic probes readily available under high pressure. To tackle this issue, we have developed a high-pressure NMR technique by using a modified Bridgman anvil cell[19] accessible to 9 GPa which covers the MIT critical pressure P_c and the superconducting phase in β-$Na_{0.33}V_2O_5$. In this Rapid Communication, we establish the magnetic P-T phase diagram of a MIT, Fig. 1(c), which demonstrates that the AF order occurs in all the pressure range where the charge order phase appears. Furthermore, we investigate the local spin susceptibility in the metallic state by the Knight-shift measurement at each V site, which shows the crossover behavior from a nearly localized metal to a Fermi-liquid metal around P_c at low temperatures. The results will give a significant insight into the MIT in quasi-1D systems and emergence of superconductivity.

The single crystals of β-$Na_{0.33}V_2O_5$ were prepared by the rf heating Czochralski method.[2] We utilized the Bridgman anvil cell with the sample space of 1.0 mmϕ in the inner diameter. The sample, $0.1 \times 0.7 \times 0.3$ mm^3, in a NMR coil was put into a Teflon cell filled with the F70-F77 fluorinate mixture oil. The leads are taken out via Au foils as shown in Fig. 1(b). We performed ^{51}V NMR measurements from 4 to 300 K up to 8.8 GPa in a constant magnetic field, 5.8709 T.

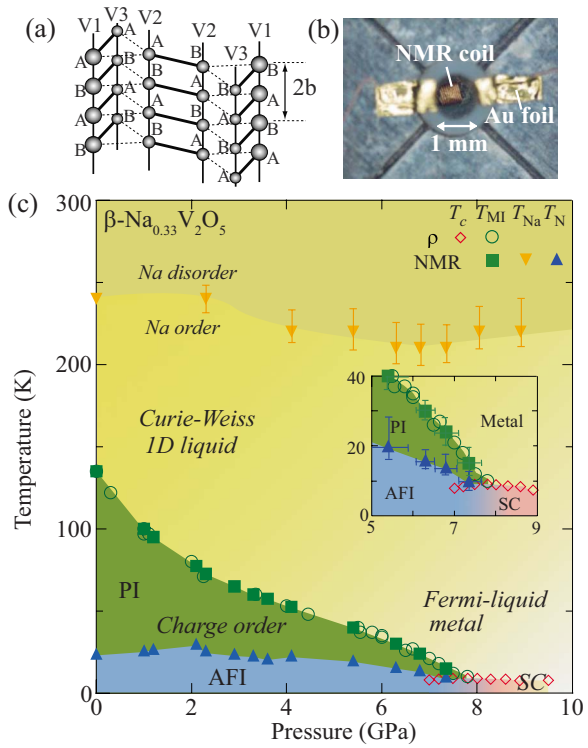

FIG. 1. (Color online) (a) Effective electronic structure in the Na-ordered metallic phase of β-$Na_{0.33}V_2O_5$. (b) A photo of the NMR coil in the Bridgman anvil cell. (c) P-T phase diagram of β-$Na_{0.33}V_2O_5$, obtained from ^{51}V NMR and resistivity measurements. ▼: T_{Na}, Na order-disorder transition temperature; ○: T_{MI}, metal-paramagnetic insulator (PI) transition temperature determined by resistivity measurements (Ref. 3); ■: T_{MI} determined by ^{51}V NMR; ▲: T_N, PI-antiferromagnetic insulator (AFI) transition temperature obtained from $1/T_2$ and spectral intensity. ◇: T_c, superconducting (SC) transition temperature, the onset of the resistivity drop (Ref. 3). Inset: magnification around the critical pressure of MIT.

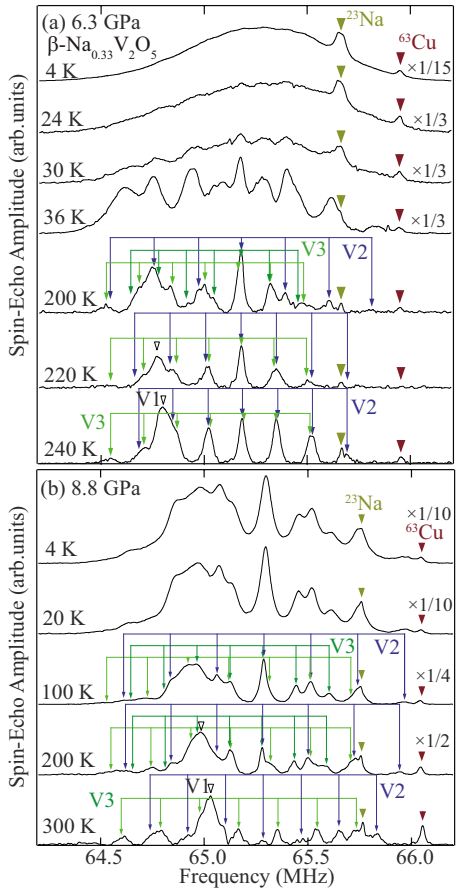

FIG. 2. (Color online) Temperature dependence of FT-NMR spectra in β-$Na_{0.33}V_2O_5$ at (a) 6.3 and (b) 8.8 GPa. Arrows denote the site assignment of three V sites and one Na site, where V2 and V3 spectra are split by the electric-quadrupole interaction.

We could not simultaneously calibrate the applied pressure P by the superconducting transition of lead[19] due to the limited sample space. Instead, the sample itself was used as a pressure gauge because the P-T_{MI} relation is known from resistivity measurements.[2] The pressure value above $P_c \sim 8$ GPa was estimated by extrapolation of the applied force F vs $P(T_{MI})$ curve, which is justified below 9 GPa.[20] Compression of the sample space forced the sample to rotate about 22° from the $-a^*$ to c axis against magnetic field below 4 GPa. The angle was estimated from a split interval $\Delta\nu$ by nuclear quadrupole interactions in ^{51}V NMR spectra. The magnetic alloy in the electrodes produced an extrinsic line broadening and a resonance shift, so we calibrated the external field from a ^{63}Cu resonance frequency with the very weak P and T dependence.[21] The spin-echo decay rate $1/T_2$ was measured at the center of the V2 lines in the Fourier-transformed (FT) spectrum.

The P-T phase diagram [Fig. 1(c)] is constructed from the T and P dependence of FT-NMR spectra and $1/T_2$ as described below. The NMR spectra obtained at the representative pressures, 6.3 and 8.8 GPa, are shown in Fig. 2. The spectrum at 300 K consists of resonance lines at ^{63}Cu, ^{23}Na, and three inequivalent ^{51}V, which are reasonably assigned from the T dependence of the shift. In Fig. 2(a), the lines staying around 65.7 and 65.9 MHz stem from the ^{23}Na site and ^{63}Cu in the NMR coil, respectively. There are two sets of V lines with the nuclear quadruple splitting into the equally spaced seven lines. One set shows no shift on cooling, while another shows a negative frequency shift. These are consistent with the behavior of V2 and V3, respectively, at ambient pressure.[9,10] The line with negligible $\Delta\nu$ (marked by open triangles) shows the largest shift to lower frequency and hence likely originates in V1. This assignment was recently confirmed by the angular variation in the spectrum[22] and consistent with the result in β-$Sr_{0.33}V_2O_5$.[23]

As temperature is lowered, the spectral profile first changes around 230–200 K, where $\Delta\nu$ of V2 increases as seen in Fig. 3(a), and the V3 lines show further splitting. These features agree with the Na order-disorder transition at T_{Na},[10,24] which doubles the unit cell along the leg (the b axis) and produces the different site potential at the A and B sites as shown in Fig. 1(a). The obtained T_{Na}, plotted as the downward triangles in Fig. 1(c), slightly decreases after a maximum around 2 GPa with increasing P.

Entering into the charge order state, the ^{51}V spectra show further splitting by tripling of the unit cell,[10] while a part of the spectra with the fast T_2 disappear. Here we determined

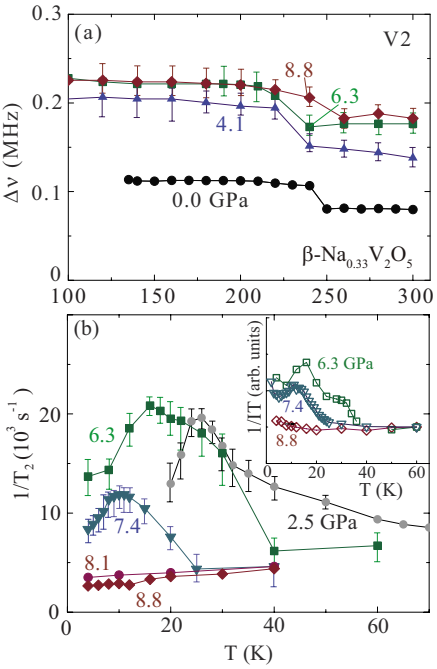

FIG. 3. (Color online) Temperature dependence of (a) $\Delta\nu$ and (b) $1/T_2$ of V2 in β-$Na_{0.33}V_2O_5$ under pressure. The inset shows the temperature dependence of $1/IT$ where I is the integrated intensity of NMR spectra.

T_{MI} as a temperature where the spectral structure smears out by the overlap of each line, e.g., ~30 K for 6.3 GPa. With increasing pressure, T_{MI} continuously decreases as seen in Fig. 1(c). For the 8.8 GPa spectra in Fig. 2(b), the broadening does not occur down to 4 K, which clearly manifests the absence of charge order. It is noted that T_{Na} remains even at P=8.8 GPa, indicating no relation between the Na and charge orders.

The spectral intensity once decreases below T_{MI} and recovers as seen in the inset of Fig. 3(b). It indicates the fastening of T_2 around the magnetic transition. The $1/T_2$ at 2.5 and 6.3 GPa actually exhibits a peak at 26 and 18 K, respectively. The obtained T_N are plotted by the upward triangles in Fig. 1(c). T_N initially increases up to 30 K (consistent with the magnetic susceptibility measurement[25]) and gradually decreases above 2.0 GPa. As T_{MI} decreases, T_N is suppressed and reaches 10 K at 7.4 GPa just below P_c.

The significant feature on the P-T phase diagram [Fig. 1(c)] is that the Néel order phase exists up to P_c. This is an ubiquitous feature in many transition-metal oxides and organic conductors.[1] In a pressure range, 7–8 GPa, the resistivity measurements imply that the charge order and superconducting phases coexist.[3] However, we could not detect the Meissner effect in the resonance frequency of the NMR tank circuit at zero field and in the ^{51}V Knight shift up to 8.8 GPa down to 2 K, probably owing to the small superconducting fraction in the inhomogeneous pressure. The simple profile of the phase diagram is in sharp contrast to the complex phase diagram of the charge order in the isostructural material β-$Sr_{0.33}V_2O_5$ where the ground state become spin singlet in the insulator phase without showing superconducting phase under pressure.[26] Comparison of the materials implies

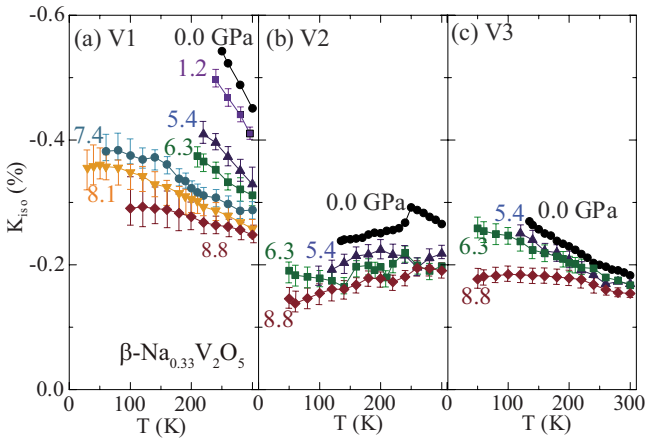

FIG. 4. (Color online) Temperature dependence of the isotropic ^{51}V Knight shifts $^{51}K_{iso}$ of (a) V1, (b) V2, and (c) V3 in the metallic state of β-$Na_{0.33}V_2O_5$ at representative pressures.

that the appearance of AF order depends on band filling and charge order pattern, possibly related to superconductivity.

An intriguing issue is the nature of the metallic state near P_c. The ^{51}V Knight shifts selectively monitor the local spin susceptibilities at the three V sites, χ_{V1}, χ_{V2}, and χ_{V3}. Here the Knight-shift tensor is anisotropic and the directions of the principal axes depend on the sites due to the anisotropic $3d$ orbital. To compare the values at the three V sites, we have evaluated the isotropic Knight shift, $^{51}K_{iso}$, from the observed shift assuming the identical shift tensor at ambient pressure.[10,22] As shown in Fig. 4, the temperature dependence of $^{51}K_{iso}$ shows remarkably contrasting behavior at the three V sites. Here the Van-Vleck contribution could be negligible because $^{51}K_{iso}$ of the V3 site was well fitted by the Curie-Weiss law without a T-invariant term.[10] The negative $^{51}K_{iso}$ stems from the negative hyperfine coupling constant governed by the core polarization from $3d$ spins. Upon cooling, $^{51}K_{iso}$ at the V1 and V3 sites, which, respectively, monitor χ_{V1} and χ_{V3}, show the Curie-Weiss-like increase in the metallic state, as if electrons were strongly localized. The incoherent metallic behavior could be ascribed to strong electron correlations by the confinement in the V1-V3 ladder. The largest shift at the V1 site suggests the largest charge density with nearly localized electrons. With increasing pressure, χ_{V1} is sensitively suppressed, while χ_{V3} is insensitive. In contrast, χ_{V2} shows nearly T-independent behavior below T_{Na} through the pressure range. The site-dependent behavior suggests that the electron itinerancy depends on the ladder—the central V2-V2 ladder seems more itinerant than the edge V1-V3 ladders. This is consistent with the larger transfer integrals in the V2-V2 ladder than the V3-V1 ladder, calculated for β-$Sr_{0.33}V_2O_5$ (Ref. 8) and β-$Na_{0.33}V_2O_5$.[27]

When the metallic state is stabilized down to low temperatures above 8 GPa, the Curie-Weiss increase in χ_{V1} and χ_{V3} levels off at low T. At the same time, the absolute values become close to each other, indicating the averaging of charge densities. The behavior can be interpreted as a crossover into the coherent Fermi-liquid metal, consistent with the T^2 behavior in resistivity.[26] In this respect, the superconducting phase appears when the Fermi-liquid coherence is devel-

oped at low temperatures and high pressures. Assuming the hyperfine coupling constant of -100 kOe/μ_B (cf. -85 kOe/μ_B for VO_2 with the valence V^{4+}),[28] the local spin susceptibilities at the three V sites are evaluated as 1.7, 1.2, and 1.3×10^{-4} emu/V i mol (i=1–3), respectively. These values are somewhat enhanced from the value evaluated by using density of states at the Fermi level at ambient pressure, 8×10^{-5} emu/V mol,[27] which would be reduced under high pressure.[29] The site dependent value is ascribed to the difference in the site potential of the Na ions.

For the AF correlations, the result of $1/T_2$ is quite intriguing. Here $T_2(\sim100\ \mu s)$ is much smaller than $T_1(\sim10$ ms),[17] so the spin-echo decay may be governed by the indirect nuclear-spin coupling rather than the T_1 process, although the echo-decay profile is close to exponential rather than Gaussian. The suppression of $1/T_2$ above P_c suggests that the AF correlations are depressed in the low-temperature metallic state.

The x-ray diffraction measurements showed that the lattice compressibility along the a and c axes, 0.4%–0.7% GPa, is much larger than that along the b axis, 0.08% GPa.[30] The pressure is hence expected to increase the interladder interactions more effectively, and hence increase the dimensionality and/or the charge transfer between the ladders. In this respect, the charge order melts by the dimensional crossover, similarly to the quasi-1D organic system.[31] The evaluation of the band filling of each ladder and the Fermi surface in the metallic state above P_c will be a key to understand the superconducting pairing interaction.

In conclusion, we revealed the magnetic pressure-temperature phase diagram in the quasi-1D β-$Na_{0.33}V_2O_5$ by developing the high-pressure NMR technique up to 9 GPa. The AF order in the charge order phase is suppressed on increasing pressure but exists until the system becomes fully metallic down to low temperatures above the critical pressure. The nearly localized electrons in the metallic state show the dimensional crossover into the Pauli paramagnetic metal with strong electron correlations under high pressures.

We appreciate fruitful discussions with M. Tsuchiizu, Y. Suzumura, and H. Seo, and also technical assistance by S. Inoue and K. Kobayashi. This work was financially supported by a Grant-in-Aid for Scientific Research (Grant No. 19014007) and Special Coordination Funds for Promoting Science and Technology from the MEXT, and also by Grants-in-Aid for Scientific Research (Grants No. 18104008, No. 19340097, and No. 19740224) from the JSPS.

[1] M. Imada, A. Fujimori, and Y. Tokura, Rev. Mod. Phys. **70**, 1039 (1998).
[2] T. Yamauchi, Y. Ueda, and N. Môri, Phys. Rev. Lett. **89**, 057002 (2002).
[3] T. Yamauchi and Y. Ueda, Phys. Rev. B **77**, 104529 (2008).
[4] H. Yamada and Y. Ueda, J. Phys. Soc. Jpn. **68**, 2735 (1999).
[5] T. Yamauchi, M. Isobe, and Y. Ueda, Solid State Sci. **7**, 874 (2005).
[6] C. Presura, M. Popinciuc, P. H. M. van Loosdrecht, D. van der Marel, M. Mostovoy, T. Yamauchi, and Y. Ueda, Phys. Rev. Lett. **90**, 026402 (2003).
[7] C. A. Kuntscher, S. Frank, I. Loa, K. Syassen, T. Yamauchi, and Y. Ueda, Phys. Rev. B **71**, 220502(R) (2005).
[8] M.-L. Doublet and M.-B. Lepetit, Phys. Rev. B **71**, 075119 (2005).
[9] M. Itoh, I. Yamauchi, T. Kozuka, T. Suzuki, T. Yamauchi, J. I. Yamaura, and Y. Ueda, Phys. Rev. B **74**, 054434 (2006).
[10] T. Suzuki, I. Yamauchi, M. Itoh, T. Yamauchi, and Y. Ueda, Phys. Rev. B **73**, 224421 (2006).
[11] M. Tsuchiizu, J. Magn. Magn. Mater. **310**, e200 (2007).
[12] M. Itoh, N. Akimoto, H. Yamada, M. Isobe, Y. Ueda, J. Phys. Soc. Jpn. Suppl. B **69**, 155 (2000).
[13] S. Nagai, M. Nishi, K. Kakurai, Y. Oohara, H. Yoshizawa, H. Kimura, Y. Noda, B. Grenier, T. Yamauchi, J. Yamaura, M. Isobe, Y. Ueda, and K. Hirota, J. Phys. Soc. Jpn. **74**, 1297 (2005).
[14] J.-I. Yamaura, M. Isobe, H. Yamada, T. Yamauchi, and Y. Ueda, J. Phys. Chem. Solids **63**, 957 (2002).
[15] A. N. Vasil'ev, V. I. Marchenko, A. I. Smirnov, S. S. Sosin, H. Yamada, and Y. Ueda, Phys. Rev. B **64**, 174403 (2001).
[16] M. Heinrich, H. A. Krug von Nidda, R. M. Eremina, A. Loidl, Ch. Helbig, G. Obermeier, and S. Horn, Phys. Rev. Lett. **93**, 116402 (2004).
[17] I. Yamauchi, M. Itoh, T. Yamauchi, and Y. Ueda, Phys. Rev. B **74**, 104410 (2006).
[18] I. Yamauchi, M. Itoh, T. Yamauchi, and Y. Ueda, J. Phys. Soc. Jpn. **77**, 104715 (2008).
[19] T. Nakanishi, N. Takeshita, and N. Môri, Rev. Sci. Instrum. **73**, 1828 (2002).
[20] H. Fukazawa, N. Yamatoji, Y. Kohri, C. Terakura, N. Takeshita, Y. Tokura, and H. Takagi, Rev. Sci. Instrum. **78**, 015106 (2007).
[21] G. B. Benedek and T. Kushida, J. Phys. Chem. Solids **5**, 241 (1958).
[22] T. Suzuki, I. Yamauchi, Y. Shimizu, M. Itoh, T. Yamauchi, and Y. Ueda (unpublished).
[23] T. Waki, M. Takigawa, T. Yamauchi, J. Yamaura, H. Ueda, and Y. Ueda, J. Phys. Chem. Solids **68**, 2143 (2007).
[24] I. Yamauchi, M. Itoh, T. Yamauchi, and Y. Ueda, Physica B **403**, 1587 (2008).
[25] G. Obermeier, D. Ciesla, S. Klimm, and S. Horn, Phys. Rev. B **66**, 085117 (2002).
[26] T. Yamauchi, H. Ueda, J. I. Yamaura, and Y. Ueda, Phys. Rev. B **75**, 014437 (2007).
[27] H. Seo, S. Ishibashi, and Y. Otsuka (unpublished).
[28] K. Takanashi, H. Yasuoka, Y. Ueda, and K. Kosuge, J. Phys. Soc. Jpn. **52**, 3953 (1983).
[29] C. Ma, R. J. Xiao, H. X. Yang, Z. A. Li, H. R. Zhang, C. Y. Liang, and J. Q. Li, Solid State Commun. **138**, 563 (2006).
[30] J. Yamaura, T. Yamauchi, E. Ninomiya, H. Sawa, M. Isobe, H. Yamada, and Y. Ueda, J. Magn. Magn. Mater. **272-276**, 438 (2004).
[31] T. Itou, K. Kanoda, K. Hiraki, T. Takahashi, K. Murata, and T. Matsumoto, Phys. Rev. B **72**, 113109 (2005).